NASA/TM–20210014330

Thermal Conductivity Estimation from Transient Test Data with Embedded Thermocouples using Genetic Algorithm Optimization

Elora Kurz and Kamran Daryabeigi
Langley Research Center, Hampton, Virginia

May 2021

NASA STI Program Report Series

Since its founding, NASA has been dedicated to the advancement of aeronautics and space science. The NASA scientific and technical information (STI) program plays a key part in helping NASA maintain this important role.

The NASA STI program operates under the auspices of the Agency Chief Information Officer. It collects, organizes, provides for archiving, and disseminates NASA's STI. The NASA STI program provides access to the NTRS Registered and its public interface, the NASA Technical Reports Server, thus providing one of the largest collections of aeronautical and space science STI in the world. Results are published in both non-NASA channels and by NASA in the NASA STI Report Series, which includes the following report types:

- TECHNICAL PUBLICATION. Reports of completed research or a major significant phase of research that present the results of NASA Programs and include extensive data or theoretical analysis. Includes compilations of significant scientific and technical data and information deemed to be of continuing reference value. NASA counterpart of peer-reviewed formal professional papers but has less stringent limitations on manuscript length and extent of graphic presentations.

- TECHNICAL MEMORANDUM. Scientific and technical findings that are preliminary or of specialized interest, e.g., quick release reports, working papers, and bibliographies that contain minimal annotation. Does not contain extensive analysis.

- CONTRACTOR REPORT. Scientific and technical findings by NASA-sponsored contractors and grantees.

- CONFERENCE PUBLICATION. Collected papers from scientific and technical conferences, symposia, seminars, or other meetings sponsored or co-sponsored by NASA.

- SPECIAL PUBLICATION. Scientific, technical, or historical information from NASA programs, projects, and missions, often concerned with subjects having substantial public interest.

- TECHNICAL TRANSLATION. English-language translations of foreign scientific and technical material pertinent to NASA's mission.

Specialized services also include organizing and publishing research results, distributing specialized research announcements and feeds, providing information desk and personal search support, and enabling data exchange services.

For more information about the NASA STI program, see the following:

- Access the NASA STI program home page at http://www.sti.nasa.gov

- Help desk contact information:

https://www.sti.nasa.gov/sti-contact-form/
and select the "General" help request type.

NASA/TM–20210014330

Thermal Conductivity Estimation from Transient Test Data with Embedded Thermocouples using Genetic Algorithm Optimization

Elora Kurz and Kamran Daryabeigi
Langley Research Center, Hampton, Virginia

National Aeronautics and
Space Administration

Langley Research Center
Hampton, Virginia 23681-2199

May 2021

Available from:

NASA STI Program / Mail Stop 148
NASA Langley Research Center
Hampton, VA 23681-2199
Fax: 757-864-6500

Abstract

Inverse heat transfer methodology previously developed to estimate thermal properties of high temperature fibrous insulation from embedded thermocouples was applied to the thermoplastic polymer, polyether-ether-ketone (PEEK). A small experimental setup was utilized to test the PEEK sample between temperatures of 300 K and 525 K at atmospheric pressure. Cylindrical plugs of PEEK with three thermocouples embedded at various depths were incorporated in the test sample. The experimental PEEK thermocouple data were used as the boundary and initial conditions of a one-dimensional numerical thermal model to predict the internal temperatures of the material. The thermal conductivity of PEEK was estimated with the Continuous Genetic Algorithm optimization technique by searching for the coefficients of a functional form of thermal conductivity that minimized the difference between the experimentally measured and model predicted internal temperature values. The thermal testing, one-dimensional numerical thermal model, optimization algorithm, analysis, and results are presented.

1 Introduction

The thermoplastic polymer, polyether-ether-ketone (PEEK) was evaluated as wind tunnel model material for hypersonic blowdown tunnels at Langley Research Center (LaRC) for global aero-heating measurements [1, 2]. Accurate temperature dependent thermal conductivity values of PEEK are needed to calculate the aero-heating rates. PEEK thermal conductivity values inferred from thermal diffusivity measurements, using the Laser Flash (LF) technique, at a commercial laboratory had been used in data reduction of wind tunnel test data, and resulted in unsatisfactory aero-heating rates. More information about LF thermal diffusivity measurements of polymers can be found in [3–5]. The purpose of this work was to estimate the temperature dependent thermal conductivity of PEEK, using the recently developed THERMal Insulation Characterization (THERMIC) test setup, and compare with the LF data. The technique utilized transient thermal testing over a large temperature range of a PEEK sample instrumented with internal thermocouples (TC). A numerical thermal model and a genetic algorithm optimization technique, the Continuous Genetic Algorithm (CGA), were used to solve the inverse heat transfer problem to estimate the thermal conductivity of PEEK from the test data.

Many methods have been developed to estimate the thermal conductivity of materials including experimental test methods and optimization methods that use a combination of test data and numerical methods to solve an inverse heat transfer problem. Standard thermal conductivity measurement techniques include steady-state methods [6, 7] that require significant test time to achieve the steady-state conditions needed to yield accurate results. Laser flash methods are also used to measure thermal diffusivity of isotropic materials and thermal conductivity is calculated using the thermal diffusivity, density, and specific heat of the material [3–5]. Optimization methods have been used in conjunction with experimental test data and a numerical heat transfer model to estimate thermal properties. The optimization techniques include gradient based, statistical, and genetic algorithms (GA). A commonly used gradient based technique is the conjugate gradient method as used by Alifanov and Mikhailov to solve an inverse heat transfer problem [8]. Scott and Beck [9] used a Gauss minimization method, that also requires the computation of gradients, with experimental test data to estimate the thermal properties of composite materials. GA methods have been applied to many heat transfer problems such as the optimization of experimental design, estimation of surface heat fluxes, and estimation of thermal properties. Many of the applications in the literature are summarized by Gosselin et al. [10]. The advantages of GAs over gradient based methods include no need to compute the gradient of the objective function, the algorithms are likely not to converge to a local minima, and the solution is less sensitive to the initial guess [10]. Thermal properties have been estimated using GAs in combination with transient and steady-state experiments. Daryabeigi applied a GA with steady-state temperature data to predict specific extinction coefficients needed for effective radiant thermal conductivity of highly porous insulation [11]. The use of transient temperature data with GA has been developed for estimating thermal properties and used in other applications such as complex aerospace structures [12, 13].

The thermal conductivity of PEEK was estimated using one set of transient temperature data, in conjunction with a one-dimensional (1D) numerical model that was incorporated into an optimization technique, CGA. CGA searches the parameter space for the coefficients of a functional form of the PEEK thermal conductivity that when used in the direct 1D numerical model, minimizes the difference between the predicted and measured temperature data. The thermal testing, numerical model, and algorithm are discussed, and results are given over the temperature range 300 K to 525 K at atmospheric pressure.

2 Thermal Testing

Thermal testing was completed at LaRC in the 0.2 m by 0.2 m transient testing apparatus, THERMIC [14]. As the name implies, THERMIC was originally designed for testing of high temperature fibrous insulation and was shown to have quasi-1D heat transfer through the center of the setup. Daryabeigi et al. modeled the heat transfer of THERMIC in 1D and the results matched center line experimental TC data throughout the depth of the sample [14]. The assembly for testing PEEK was comprised of the components shown in Fig. 1.

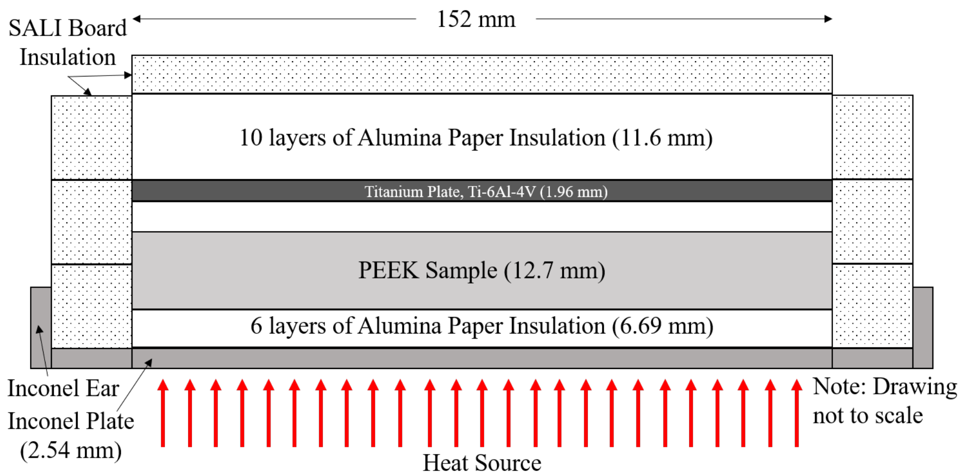

Figure 1: Components of THERMIC setup for PEEK testing with thickness measurements.

An Inconel (Inc) plate was the base of the setup with four TCs on the top side, away from the heat source. One TC was placed in the center of the plate with two others offset diagonally from the center by 35.4 mm. The fourth TC was located on the opposite diagonal 53.2 mm from the center. Above the Inc plate were six layers of Alumina Paper (APA), a high temperature fibrous insulation felt, with a TC installed in the middle of the felt squares between every two layers. The PEEK plate was placed above the six layers of APA. Another four layers of APA were placed above the PEEK plate with one TC in the middle of the four layer stack-up. A Titanium (Ti) plate that was instrumented with six TCs was located above the four layers of APA. Ten layers of APA were located above the Ti plate followed by SALI Board, a rigid insulation board, which was placed above the APA to reduce heat loss from the top of the apparatus. The entire setup was placed in SALI Board picture frames to minimize lateral heat losses. The heat source was a standard Meker burner, shown in Fig. 2, located below the setup and supplied with propane gas with the flow rate controlled by a valve.

Traditionally, the THERMIC setup has been used to test samples that are not affected by the high temperatures the Inc plate can experience during testing and the material that is being tested can sit directly above the Inc plate. However, PEEK has a melting point temperature of about 600 K. APA was placed between the Inc and PEEK to reduce the heat transfer to the PEEK plate. A simple 1D thermal analysis was completed to determine that four layers of APA would be needed to keep the PEEK plate from experiencing temperatures above 550 K. The other components of the setup, Ti plate, SALI Board, and other APA layers were a part of the original THERMIC setup and were kept intact. More details about THERMIC can be found in [14].

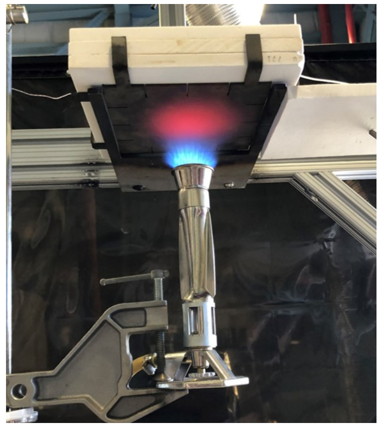

Figure 2: THERMIC setup with Meker burner during a test.

The PEEK plate was instrumented with 15 TCs. The six surface TCs and nine internal TCs are shown in Fig. 3. The internal PEEK TCs were placed by removing three cylindrical portions (plugs) from the plate. Similar plug instrumentation was used in [15–17]. Each plug is 7.9 mm in diameter and 12.7 mm in length. Three 10 mm metal-sheathed type K TCs were installed through the thickness of each plug.

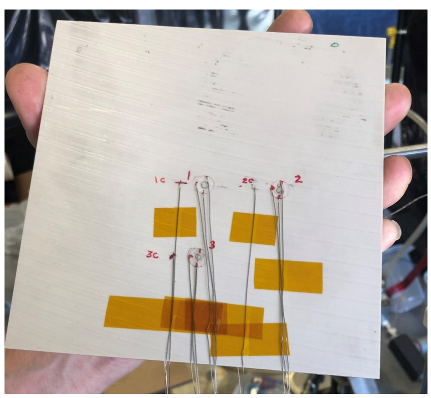

(a) PEEK Plate

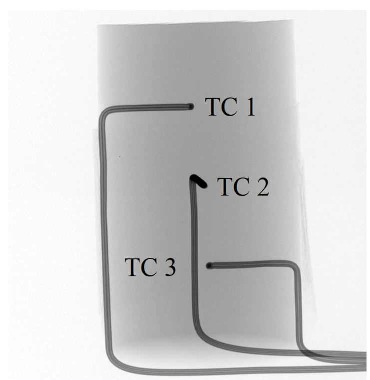

(b) PEEK Plug with TCs

Figure 3: PEEK sample plate with (a) external TCs and (b) CT image of internal plug TCs.

The internal TCs, three per plug, were placed through the thickness every 3.18 mm. A CT image of a plug with internal TCs is shown in Fig. 3b. Six surface TCs, three on top and three on bottom, were placed next to each plug on the plate. Small holes were drilled from the side of each plug to the center and the TCs were inserted. Plug 1 was placed in the direct center of the plate, and plugs 2 and 3 were offset 31.75 mm from the center. A Computerized Tomography (CT) scanner was used to verify through-thickness depths of each TC for use in the analysis. The depth measurements of each plug are given in Table 1 and were used in 1D numerical analysis.

Table 1: TC depth measurements from the top (hot side) of each plug taken from CT scans.

Plug	**TC 1**	**TC 2**	**TC 3**
1	3.30 mm	6.25 mm	9.53 mm
2	3.14 mm	6.21 mm	9.74 mm
3	3.26 mm	6.46 mm	9.39 mm

Five thermal tests of the PEEK plate were conducted to show repeatability of testing even though data from only one test was needed to estimate the thermal conductivity of PEEK over the entire 300 K to 525 K temperature range. The temperatures from the hot side of the PEEK plate for all five tests are shown in Fig. 4.

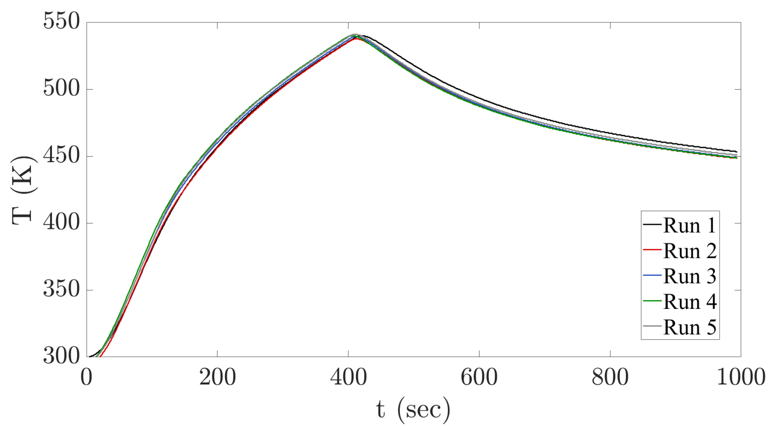

Figure 4: Temperature data from hot side of PEEK plate during all five tests.

For each test, heat was applied for approximately seven minutes which resulted in an average PEEK maximum temperature of 540 K. Temperature data was collected during heating and for approximately 15 minutes after heat was turned off. The Meker burner uniformly heated the Inc plate with an average difference of 1.0 percent between the three central TCs. The PEEK was also uniformly heated with an average difference of 0.9 percent between the three TCs on the hot side of the sample. The temperature uniformity on the Inc plate and PEEK sample indicate the heat transfer through the center of the setup is quasi-1D. Temperatures from a sample test are shown in Fig. 5. Inc is the average temperature of the four TCs on the Inconel plate. APA_2 and APA_4 is the temperature from the thermocouple on top of APA layer two and four respectively. The PEEK plate temperatures for plug one are denoted as PEEK. APA_6 is the temperature on top of the sixth layer of APA, between the PEEK plate and the titanium plate. Ti is the average of four central TCs on the cold side of the titanium plate.

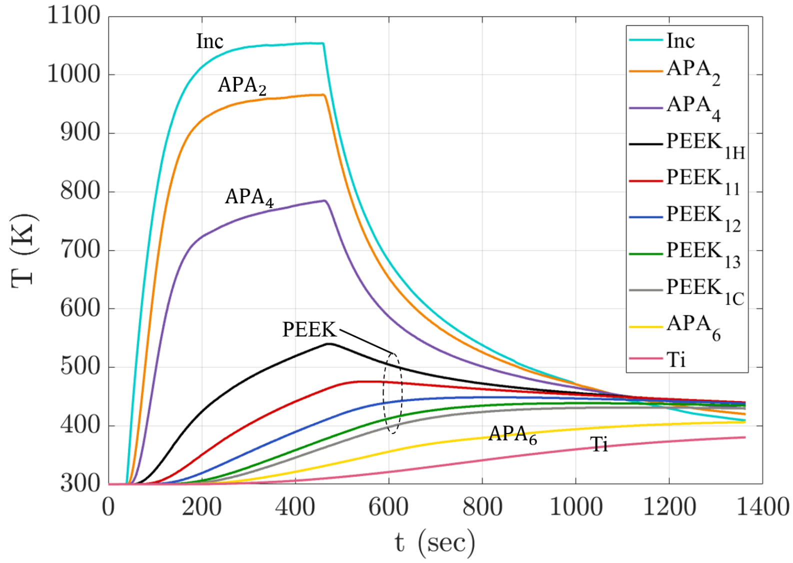

Figure 5: Thermocouple data from the THERMIC setup during PEEK testing.

3 Thermal Model

The internal temperatures of the PEEK plate were approximated with a numerical solution of the transient heat conduction partial differential equation (PDE), Eq. 1, in 1D.

$$\begin{aligned}
\frac{\partial}{\partial x}\left(k(u)\frac{\partial u}{\partial x}\right) &= \rho c_p(u)\frac{\partial u}{\partial t}, && 0 < x < L \\
u(x,0) &= f(x), && 0 \leq x \leq L \\
u(0,t) &= g(t), && 0 < t \\
u(L,t) &= h(t), && 0 < t
\end{aligned} \tag{1}$$

where $u(x,t)$ is the temperature at location x and time t, $k(u)$ is the thermal conductivity of PEEK as a function of temperature, ρ is the density of PEEK, and $c_p(u)$ is the specific heat of PEEK as a function of temperature. An energy balance finite difference scheme with the Crank-Nicolson time marching method [18] along with a tridiagonal system solver, the Thomas Algorithm [19] were used to get the approximate solution, $\hat{u}$, at each time step. The initial condition, $f(x)$, was interpolated data from the initial temperatures of the PEEK plate. The Dirichlet boundary conditions, $g(t)$ and $h(t)$, were specified from measured temperature data on the hot and cold sides of the PEEK plate respectively. The center plug, plug 1, was used in the analysis. Nodal locations that represent TC locations in the PEEK are denoted, $PEEK_{11}, PEEK_{12}, PEEK_{13}$, where the first subscript number represents the plug and the second subscript number represents the through thickness TC location with one being closest to the heat source. The model domain in relation to the TCs in the experimental setup is shown in Fig. 6.

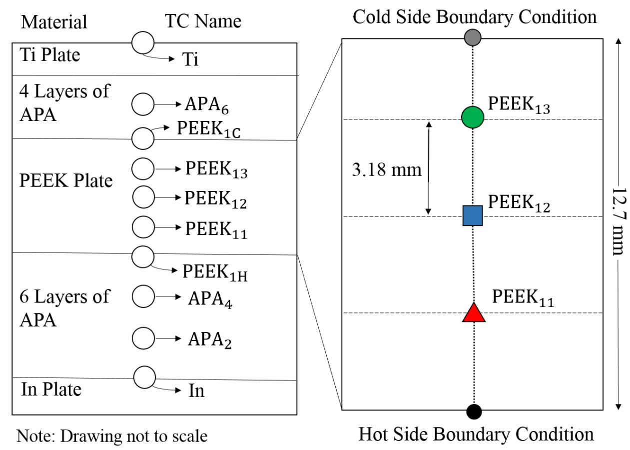

Figure 6: THERMIC TCs and corresponding PEEK numerical model domain and nodal locations.

A nodal convergence study was performed to determine that 65 nodes, with a nodal spacing of 0.198 mm, was adequate for the analysis. A time step of one second was used to match the data acquisition rate. The thermal conductivity of PEEK was estimated with CGA and the other thermal properties, $c_p(u)$ and ρ, were assumed known. Specific heat,

$$c_p(u) = 1.0477 \times 10^{-5}u^3 - 6.1332 \times 10^{-3}u^2 + 3.3066u + 3.3606 \times 10^2, \qquad (2)$$

was a polynomial curve fit to measured data from a differential scanning calorimeter at LaRC and density, $\rho = 1264$ $(\frac{kg}{m^3})$, was from measurements at a commercial laboratory [20]. The thermal conductivity, $k(u)$, was estimated using CGA.

4 Thermal Conductivity Estimation

The thermal conductivity of PEEK was estimated by solving the inverse heat transfer problem using the CGA optimization technique [21]. Some advantages of CGA over other optimization techniques are an initial guess is not required, and the algorithm has the ability to find the global minimum when the parameter space has many local minima. The goal of the algorithm was to find the set of coefficients for a functional form of thermal conductivity, that when used in the numerical model, best minimized the difference between the measured experimental temperatures and the predicted numerical model temperatures. The thermal conductivity of PEEK was assumed to be a third order polynomial function of temperature

$$k(u) = c_0 + c_1u + c_2u^2 + c_3u^3. \qquad (3)$$

The coefficients, c_i $i \in \{0, 1, 2, 3\}$, were assumed to be in the intervals

$$c_0 \in [-10^{-1}, 10^{-1}]$$
$$c_1 \in [-10^{-4}, 10^{-4}]$$
$$c_2 \in [-10^{-8}, 10^{-8}]$$
$$c_3 \in [-10^{-10}, 10^{-10}].$$

CGA was used to search the parameter space for the set of coefficients that best minimized the objective function,

$$z(\hat{u}) = \sum_{j=1}^{m} \sum_{i=1}^{n} \left(\frac{P(i,j) - \hat{u}(i,j)}{\hat{u}(i,j)} \right)^2, \tag{4}$$

where P is the PEEK measured temperatures at the internal TCs, $PEEK_{11}$, $PEEK_{12}$, and $PEEK_{13}$. P can either be a vector of temperatures from one TC location or a matrix of multiple internal TC locations. $\hat{u}$ is the resulting numerical temperature solution at the nodes corresponding to the selected TC locations in P when using a set of coefficients in the thermal conductivity function, Eq. 3. The index m is the number of internal TC locations selected and n is the number of time steps.

CGA begins by constructing a matrix of initial coefficient sets by selecting a uniform distribution of random numbers within the specified intervals. The algorithm then uses each set as the coefficients of a functional form of the PEEK thermal conductivity, and then temperature values through the domain are obtained with the 1D heat conduction model using each thermal conductivity set of coefficients. The objective function is evaluated using the numerical temperature values from the nodal locations corresponding to the PEEK TCs selected for comparison and an objective function value is received for each set of coefficients. The sets are ordered based on their objective function values, from smallest to largest since the algorithm is trying to minimize the objective function. The top fifty percent of sets that best minimized the objective function are selected to create new coefficient sets by performing single point crossover [21] as shown in Fig 7.

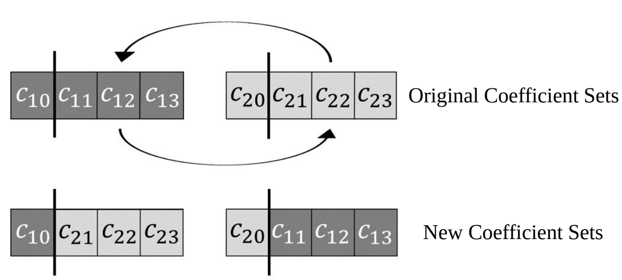

Figure 7: Example of single point crossover performed on a pair of coefficient sets.

The new sets of coefficients are combined with the original top 50 percent of the population to create the new population. Then, a percentage of the new population is mutated to add variety to the possible solutions. The mutations are performed by randomly selecting a percentage of individual coefficients and replacing each coefficient with a value within the given intervals. The mutations allow the algorithm to search in other areas and shift out of possible local minima in the parameter space. The process continues until one of two stopping criteria are met. The algorithm terminates if the maximum number of iterations has been met or if the objective function value is below the specified threshold. If neither condition is met, the algorithm continues on for another iteration by evaluating the model and objective function for the new population. The result is a set of coefficients that minimize the objective function within the allotted number of iterations. The steps in CGA from [21] are shown in Fig. 8. More information about the application of CGA to thermal property estimation can be found in [22].

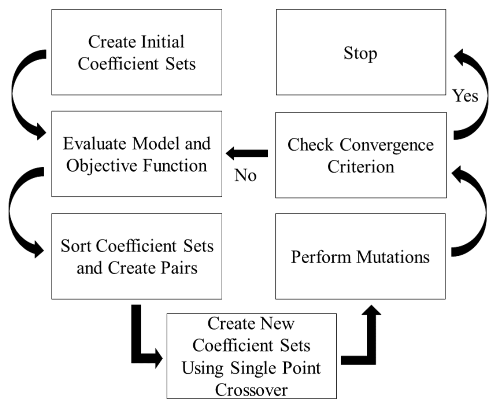

Figure 8: The Continuous Genetic Algorithm flow chart.

5 Results

The thermal conductivity of PEEK was estimated over the temperature range of 300 K to 525 K at atmospheric pressure. The PEEK temperature data from a typical test using the THERMIC setup is shown in Fig. 9. The solid black line, $PEEK_{1H}$, was used as the hot side Dirichlet boundary condition in the 1D numerical model. The dashed gray line, $PEEK_{1C}$, was used as the cold side Dirichlet boundary condition. The initial temperature of the PEEK plate was spatially interpolated and used as the initial condition. The red triangle, blue square, and green circle lines are the internal PEEK temperatures that were used as P in the objective function, Eq. 4.

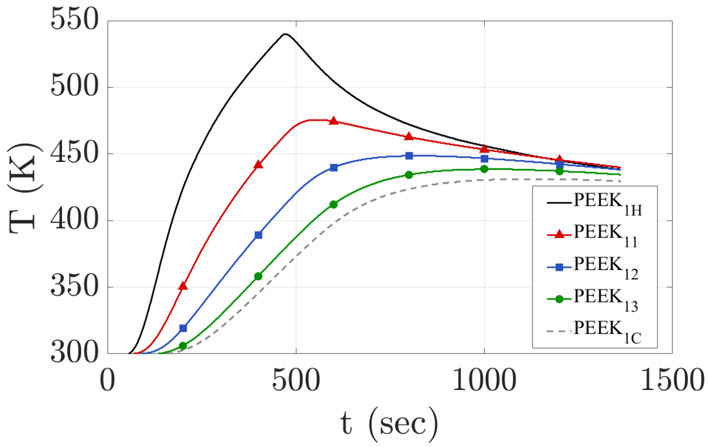

Figure 9: Sample experimental PEEK plate temperatures within THERMIC setup.

The temperature data was used in conjunction with CGA to estimate the thermal conductivity of PEEK. Four estimates were calculated, one estimate using each of the three internal PEEK TC individually and one estimate using all three TCs simultaneously as P in Eq. 4. The convergence criteria used for the CGA was a maximum number of iterations of 500 and a threshold value of 0.01 for the objective function. A maximum number of iterations of 500 was selected from author's previous experience using the algorithm to estimate thermal conductivity of materials. The algorithm commonly terminated because the maximum number of iterations was met. The coefficient ranges were perturbed if any of the solutions were on the boundary of their intervals when the maximum number of iterations were met. The coefficients that best minimized the objective function within the allowed number of iterations were found. The temperature-dependent PEEK thermal conductivity CGA estimates are shown in Fig. 10 compared to prior PEEK thermal conductivity data that had been obtained from LF thermal diffusivity data [3]. The legend PEEK subscripts denote the different thermal conductivity values. The subscripts 11, 12, and 13 are CGA estimates using the individual PEEK TCs, ALL is the CGA estimate using data from all three PEEK TCs simultaneously, and LF is the thermal conductivity from the laser flash measurement.

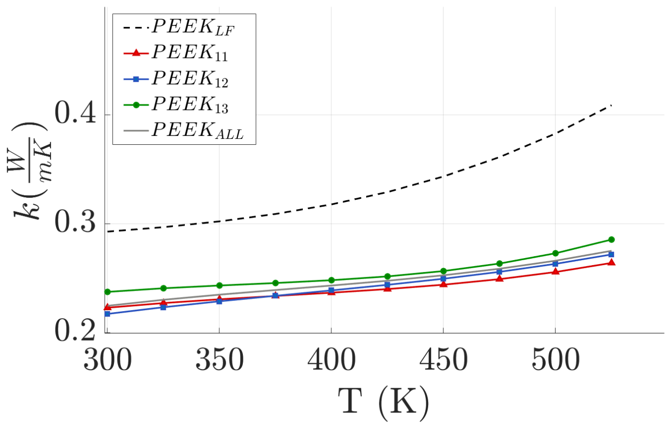

Figure 10: PEEK thermal conductivity estimates as a function of temperature at each TC location compared to LF data.

The PEEK thermal conductivity estimates from each TC location individually and all three collectively differed by about three percent. Since all estimates were similar, the estimate using all TC locations was chosen as the final PEEK thermal conductivity estimate and is shown in Fig. 11. The CGA estimate was approximately 35 percent lower than the LF PEEK thermal conductivity values. The final CGA thermal conductivity coefficient values are given in Table 2.

Other PEEK thermal conductivity values that are close to the CGA estimate were found in the literature. Rivière et al. measured PEEK thermal conductivity using a modulated-temperature differential scanning calorimetry technique that resulted in values of approximately 0.26 $\frac{W}{mK}$ to 0.27 $\frac{W}{mK}$ over the temperature range of 293 K to 323 K [23]. Stepashkina et al. used the laser flash technique and found PEEK thermal conductivity to be approximately 0.26 $\frac{W}{mK}$ to 0.29 $\frac{W}{mK}$ over the temperature range 298 K to 573 K [24]. Díez-Pascual et al. reported a room temperature PEEK thermal conductivity of approximately 0.23 $\frac{W}{mK}$ [25].

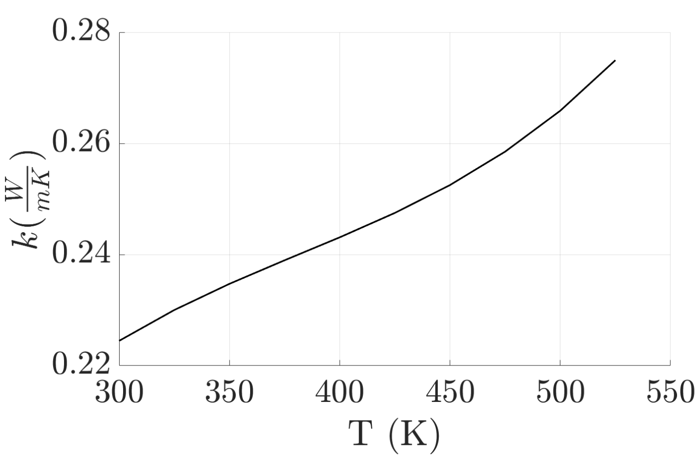

Figure 11: PEEK thermal conductivity estimate as a function of temperature.

Table 2: CGA estimate of PEEK thermal conductivity coefficients for Eq. 3

$\mathbf{c_0}$	$\mathbf{c_1}$	$\mathbf{c_2}$	$\mathbf{c_3}$
-4.0607×10^{-2}	1.8749×10^{-3}	-4.4753×10^{-6}	3.9027×10^{-9}

6 Analysis of Results

The PEEK thermal conductivity estimate using temperature data from the THERMIC testing apparatus with a 1D numerical model and the CGA optimization technique differed from the LF data on average by 35 percent. With a large difference in the values, a comparison was done to evaluate how the CGA estimate and inferred LF thermal conductivity values, when used in the numerical model, match the internal temperature data of all three plugs. The LF and CGA thermal conductivity values were used in the PEEK 1D numerical model with the given initial and boundary conditions from the experimental temperature data which resulted in two sets of predicted temperatures for each plug. The predicted temperatures were then compared to the measured experimental temperature data using a percent difference given by

$$\Delta T_{ij} = 100\frac{|\hat{u}_{ij} - P_{ij}|}{P_{ij}},\ i, j \in \{1, 2, 3\}, \tag{5}$$

where i is the plug number and j is the TC location with one being closest to the heat, three furthest away from the heat, and two in the middle. $\hat{u}_{ij}$ is the numerical model temperature prediction for plug i at the node corresponding to TC location j. P_{ij} is the PEEK experimental temperature data at plug i and TC location j. A breakdown of how the LF and CGA PEEK thermal conductivity estimates are compared is given in Fig. 12. First, the two thermal conductivity estimates, k_{CGA} and k_{LF}, were used as the PEEK thermal conductivity in the direct numerical model. The resulting temperature values from each model, $\hat{u}_{CGA}$ and $\hat{u}_{LF}$, are then used in Eq. 5. The resulting ΔT values for plug one, two, and three are shown in Figs. 13, 14, and 15 respectively.

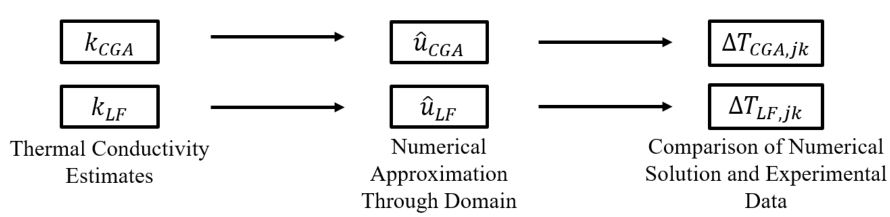

Figure 12: Flowchart of CGA and LF thermal conductivity comparison steps.

The difference between the predicted temperature values using the the LF thermal conductivity values and the experimental temperature data for plug one is shown in Fig. 13a. The difference between the predicted temperature values using the CGA estimated thermal conductivity and the experimental temperature data for plug one is shown in Fig. 13b. The LF thermal conductivity gave an average percent difference between the predicted and experimental temperatures of 1.4 percent and a maximum percent difference of 3.6 percent. The CGA thermal conductivity estimate gave an average percent difference between the predicted and experimental temperatures of 0.2 percent and a maximum percent difference of 1.4 percent.

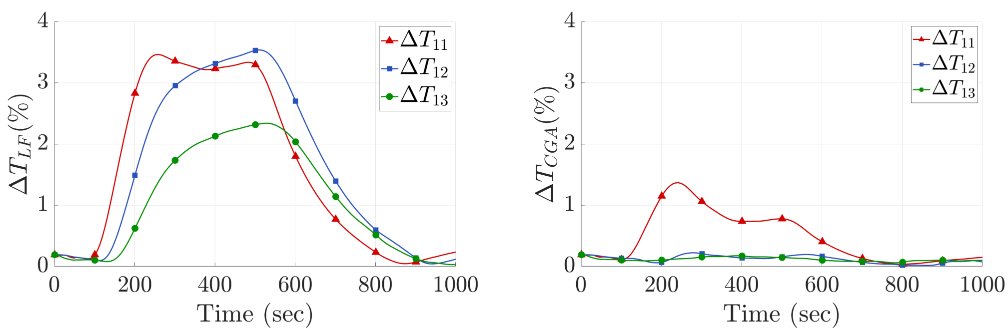

(a) (b)

Figure 13: Temperature differences between experimental and predicted model values of plug one using thermal conductivity estimates (a)LF estimate and (b) CGA estimate.

All of the CGA thermal conductivity estimates were obtained with data from the center plug in the PEEK plate, plug one. To further compare the LF thermal conductivity values and the CGA estimate, the same temperature differences, Eq. 5, were calculated for the off-center plugs. The temperature difference at the nodal locations that correspond to the TC locations for the LF thermal conductivity estimate and CGA estimate for plug two and three are shown in Figs. 14 and 15 respectively. The LF thermal conductivity estimate gave an average percent difference between the plug two predicted and measured temperatures of 1.8 percent and a maximum percent difference of 3.5 percent. The CGA thermal conductivity estimate gave an average percent difference between the plug two predicted and measured temperatures of 0.7 percent and a maximum percent difference of 1.3 percent.

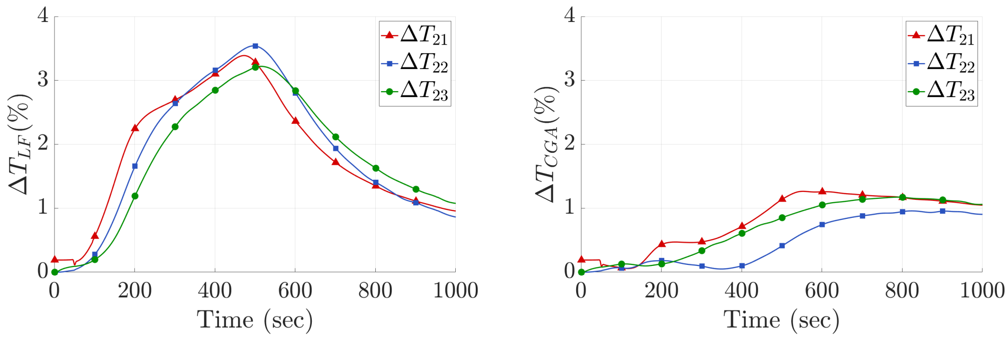

(a) (b)

Figure 14: Temperature differences between measured and predicted model values of plug two using thermal conductivity estimates (a) LF estimate and (b) CGA estimate.

The middle TC of plug three, TC_{32}, malfunctioned during testing thus the TC is not shown in Fig. 15. The predicted temperature data using the LF thermal conductivity values had an average percent difference compared to the measured temperature data of 1.0 percent and a maximum percent difference of 2.6 percent. The predicted temperature data using the new CGA thermal conductivity values had an average percent difference compared to the measured temperature data of 0.2 percent and a maximum percent difference of 0.5 percent.

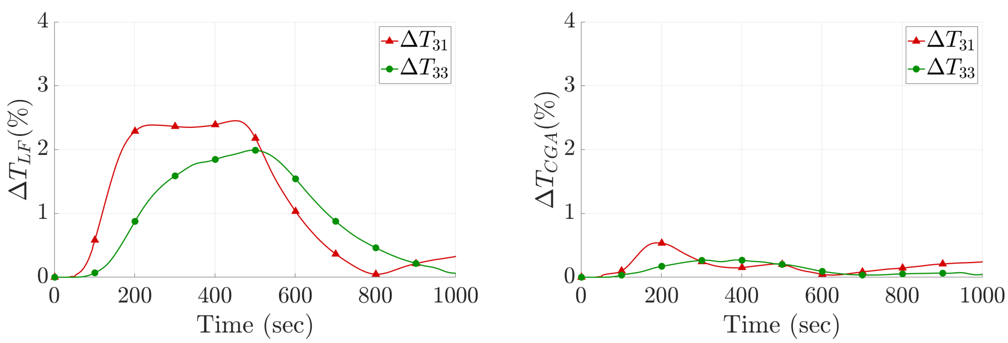

(a) (b)

Figure 15: Temperature differences between measured and predicted model values of plug three using thermal conductivity estimates (a) LF estimate and (b) CGA estimate.

The CGA thermal conductivity estimate resulted in lower temperature differences for all three plugs compared to the LF thermal conductivity. Overall, the CGA PEEK thermal conductivity estimate reduced the percent error more than half compared to the LF PEEK thermal conductivity for all three plugs. The average percent difference when using the LF thermal conductivity was 1.4 percent compared to the CGA estimate that gave an average percent difference over all three plugs of 0.3 percent.

7 Concluding Remarks

Thermal conductivity of the thermoplastic polymer PEEK was estimated using a combination of transient experimental temperature data, a 1D numerical thermal model, and the CGA optimization technique. Internal temperature data of PEEK was measured using instrumented plugs with TCs at various depths. The temperature data was used in combination with a 1D finite difference numerical model to replicate the heat conduction in the PEEK. The thermal property estimates were obtained by solving the inverse heat transfer problem using the CGA optimization technique to search the parameter space for coefficients of a functional form of the thermal conductivity. The algorithm used a set of the possible coefficient solutions in the direct numeral model to estimate the internal PEEK temperatures. The temperature values predicted by the numerical model were then compared to the experimental data from the internal PEEK plate TCs. The algorithm found the set of coefficients that best minimized the difference between the predicted and measured temperature values.

The resulting CGA thermal conductivity estimate, over the 300 K to 550 K temperature range, was 35 percent lower than the previously obtained LF thermal conductivity values. The CGA thermal conductivity estimate was then compared to the LF thermal conductivity values by using the estimates in a direct numerical model and comparing predicted temperature data to the measured experimental data for the three plugs within the PEEK plate. The LF thermal conductivity estimate resulted in percent differences ranging from 1.0 percent to 1.8 percent with an average of 1.4 percent at all TC locations for all plugs. The CGA thermal conductivity estimate was shown to have an average percent difference at all TC locations for all plugs of 0.3, ranging from 0.2 percent to 0.7 percent. The CGA thermal conductivity estimate resulted in smaller error compared to the LF thermal conductivity data when used in the numerical thermal analysis for all plugs. The reduction in error will allow for more accurate aero-heating rates.

References

[1] Berry, S.; and Berger, K.: "NASA Langley Experimental Aerothermodynamic Contributions to Slender and Winged Hypersonics Vehicles", AIAA 2015-0213, January 2015.

[2] Berry, S.; Mason, M.; Greene, F.; King, R.; Rieken, E.; and Basore, K.: "LaRC Aerothermodynamic Ground Tests in Support of BOLT Flight Experiment", AIAA 2019-0091, January 2019.

[3] ASTM-E1461-13: "Standard Test Method for Thermal Diffusivity by the Flash Method", ASTM International, 2013.

[4] Sombatsompop, N.; and Wood, A. K.: "Measurement of Thermal Conductivity of Polymers using an Improved Lee's Disc Apparatus", *Polymer Testing*, vol. 16, no. 3, June 1997.

[5] Santos, W. N.; Mummery, P.; and Wallwork, A.: "Measurement of Thermal Conductivity of Polymers using an Improved Lee's Disc Apparatus", *Polymer Testing*, vol. 24, no. 5, August 2005.

[6] ASTM-C177-13: "Standard Test Method for Steady-State Heat Flux Measurements and Thermal Transmission Properties by Means of the Guarded-Hot-Plate Apparatus", ASTM International, 2013.

[7] ASTM-C518-17: "Standard Test Method for Steady-State Thermal Transmission Properties by Means of the Heat Flow Meter Apparatus", ASTM International, 2017.

[8] Alifanov, O.; and Mikhailov, V.: "Solution of Nonlinear Inverse Thermal Conductivity Problem by the Iteration Method", *Journal of Engineering Physics*, vol. 35, no. 6, Dec. 1978, pp. 1501–1506.

[9] Scott, E.; and Beck, J.: "Estimation of thermal properties in carbon/epoxy composite materials during curing", *Journal of Composite Materials*, vol. 26, no. 1, 1992, pp. 20–36.

[10] Gosselin, A.; Tye-Gingras, M.; and Mathieu-Potvin, F.: "Review of Utilization of Genetic Algorithms in Heat Transfer Problems", *International Journal of Heat and Mass Transfer*, vol. 52, no. 9-10, April 2009, pp. 2169–2188.

[11] Daryabeigi, K.; Cunnington, G.; and Knutson, J.: "Combined Heat Transfer in High-Porosity High-Temperature Fibrous Insulation: Theory and Experimental Validation", *International Journal of Thermophysics*, vol. 25, no. 4, Oct.-Dec. 2011, pp. 536–546.

[12] Hanuska, A.; Scott, E. P.; and Daryabeigi, K.: "Thermal Characterization of Aerospace Structures", *Journal of Thermophysics and Heat Transfer*, vol. 14, no. 3, July-Sept. 2000.

[13] Garcia, S.; Guynn, J.; and Scott, E.: "Use of Genetic Algorithms in Thermal Property Estimation: Part II—Simultaneous Estimation of Thermal Properties", *Numerical Heat Transfer*, vol. 33, no. 2, 1998.

[14] Daryabeigi, K.; Blosser, M. L.; Geouge, W. D.; and Cheatwood, J. S.: "A Simple Transient Thermal Test Assembly for Insulation Materials", NASA TM-2019-220249, 2019.

[15] Pizzo, M.; Glass, D.; and Bey, K.: "Analysis of Internal Thermocouple Data in Carbon/Carbon Using Inverse Heat Conduction Methods", AIAA 2016-0508, January 2016.

[16] Gazarik, M. J.; Wright, M. J.; Little, A.; Cheatwood, F. M.; Herath, J. A.; Munk, M. M.; Novak, F. J.; and Martinez, E. R.: "Overview of the MEDLI Project", *2008 IEEE Aerospace Conference*, 2008, pp. 1–12.

[17] Hwang, H.; Bose, D.; Wright, H.; White, T.; Schoenenberger, M.; Santos, J.; Karlgaard, C.; Kuhl, C.; Oishi, T.; and Trombetta, D.: "Mars 2020 Entry, Descent, and Landing Instrumentation (MEDLI2)", AIAA 2016-3536, June 2016.

[18] Bradie, B.: *A Friendly Introduction to Numerical Analysis*, Pearson Prentice Hall, 2006.

[19] Thomas, L.: Elliptic Problems in Linear Differential Equations over a Network, Watson Science Computer Lab Report, 1949.

[20] Netzsch: Report Number 621004797, July 2019.

[21] Haupt, R. L.; and Haupt, S. E.: *Practical Genetic Algorithms*, Wiley, 1998.

[22] Frye, E.; and Darayabeigi, K.: "Thermal Property Estimation of Fibrous Insulation: Heat Transfer Modeling and the Continuous Genetic Algorithm", AIAA 2019-1279, January 2019.

[23] Rivière, L.; Causse, N.; Lonjon, A.; Dantras, E.; and Lacabanne, C.: "Specific heat capacity and thermal conductivity of PEEK/Ag nanoparticles composites determined by Modulated Temperature Differential Scanning Calorimetry", *Polymer Degradation and Stability*, vol. 127, 2016.

[24] Stepashkina, A. A.; Chukova, D. I.; Senatova, F. S.; Salimonac, A. I.; Korsunskybc, A. M.; and Kaloshkina, S.: "3D-printed PEEK-carbon fiber (CF) composites: Structure and thermal properties", *Composite Science and Technology*, vol. 164, August 2018.

[25] Díez-Pascual, A. M.; Naffakh, M.; González-Domínguez, J. M.; Ansón, A.; Martínez-Rubi, Y.; Martínez, M. T.; Simard, B.; and Gómez, M. A.: "High performance PEEK/carbon nanotube composites compatibilized with polysulfones-II. Mechanical and electrical properties", *Carbon*, vol. 48, no. 12, October 2010.

REPORT DOCUMENTATION PAGE	*Form Approved OMB No. 0704–0188*

1. REPORT DATE *(DD-MM-YYYY)*
01-04-2021

2. REPORT TYPE
Technical Memorandum

3. DATES COVERED *(From - To)*

4. TITLE AND SUBTITLE
Thermal Conductivity Estimation from Transient Test Data with Embedded Thermocouples using Genetic Algorithm Optimization

5a. CONTRACT NUMBER

5b. GRANT NUMBER

5c. PROGRAM ELEMENT NUMBER

6. AUTHOR(S)
Kurz, Elora; Daryabeigi, Kamran

5d. PROJECT NUMBER

5e. TASK NUMBER

5f. WORK UNIT NUMBER

7. PERFORMING ORGANIZATION NAME(S) AND ADDRESS(ES)
NASA Langley Research Center
Hampton, Virginia 23681-2199

8. PERFORMING ORGANIZATION REPORT NUMBER
–

9. SPONSORING/MONITORING AGENCY NAME(S) AND ADDRESS(ES)
National Aeronautics and Space Administration
Washington, DC 20546-0001

10. SPONSOR/MONITOR'S ACRONYM(S)
NASA

11. SPONSOR/MONITOR'S REPORT NUMBER(S)
NASA/TM–20210014330

12. DISTRIBUTION/AVAILABILITY STATEMENT
Unclassified-Unlimited
Subject Category 34
Availability: NASA STI Program (757) 864-9658

13. SUPPLEMENTARY NOTES

14. ABSTRACT
Inverse heat transfer methodology previously developed to estimate thermal properties of high temperature fibrous insulation from embedded thermocouples was applied to the thermoplastic polymer, polyether-ether-ketone (PEEK). A small experimental setup was utilized to test the PEEK sample between temperatures of 300 K and 525 K at atmospheric pressure. Cylindrical plugs of PEEK with three thermocouples embedded at various depths were incorporated in the test sample. The experimental PEEK thermocouple data were used as the boundary and initial conditions of a one-dimensional numerical thermal model to predict the internal temperatures of the material. The thermal conductivity of PEEK was estimated with the Continuous Genetic Algorithm optimization technique by searching for the coefficients of a functional form of thermal conductivity that minimized the difference between the experimentally measured and model predicted internal temperature values. The thermal testing, one-dimensional numerical thermal model, optimization algorithm, analysis, and results are presented.

15. SUBJECT TERMS
Thermal Properties, Optimization, Thermal Modeling, Thermal Testing

16. SECURITY CLASSIFICATION OF: a. REPORT	b. ABSTRACT	c. THIS PAGE	17. LIMITATION OF ABSTRACT	18. NUMBER OF PAGES	19a. NAME OF RESPONSIBLE PERSON
U	U	U	UU	22	STI Information Desk (help@sti.nasa.gov)
					19b. TELEPHONE NUMBER *(Include area code)* (757) 864-9658

Standard Form 298 (Rev. 8/98)
Prescribed by ANSI Std. Z39.18